

PDF hosted at the Radboud Repository of the Radboud University Nijmegen

The following full text is a publisher's version.

For additional information about this publication click this link.

<http://hdl.handle.net/2066/21940>

Please be advised that this information was generated on 2017-12-05 and may be subject to change.

Technical Note

Elimination of Autofluorescence in Immunofluorescence Microscopy with Digital Image Processing¹

CHRIS H. A. VAN DE LEST, ELLY M. M. VERSTEEG, JACQUES H. VEERKAMP,
and TOIN H. VAN KUPPEVELT²

Department of Biochemistry, University of Nijmegen, Nijmegen, The Netherlands.

Received for publication November 16, 1994 and in revised form February 22, 1995; accepted February 25, 1995 (4T3538).

Autofluorescence can be a very disturbing factor in immunofluorescence microscopy. We present here a method to eliminate autofluorescence. The method is based on the fact that most autofluorescent compounds have broad-banded excitation and emission spectra, whereas specific fluorescent probes have narrow spectra. Two images are recorded and digitized, one at a wavelength exciting both the fluorescent probe and the autofluorescent molecules, and one at a wavelength exciting only the latter. Subtraction of the autofluorescence signal from the total fluorescence signal, using a self-developed computer program, results in an autofluorescence-

free image. The procedure is demonstrated for elimination of elastin-derived autofluorescence in human lung alveoli and for elimination of lipofuscin-derived autofluorescence in human heart muscle. The autofluorescence signal is positively correlated with tissue section thickness ($r = 0.93$; $p < 0.0001$), and can be used to correct the specific fluorescence signals for section thickness. (*J Histochem Cytochem* 43:727-730, 1995)

KEY WORDS: Autofluorescence; Digital image analysis; Immunofluorescence microscopy; Elastin; Lipofuscin.

Introduction

Autofluorescence is a very common phenomenon and can interfere in microscopic studies using fluorescence labeling. It is caused by certain biomolecules, such as elastin, fibronectin, and lipofuscin, and by aldehyde fixation (1). Autofluorescence can be very intense and often results in masking of the specific fluorescence signals. Only a few reports have dealt with the elimination of autofluorescence, most of them related to flow cytometry. Addition of crystal violet, for example, has been used to quench autofluorescence of macrophages in flow cytometry (2). Dual-wavelength flow cytometry has also been applied to correct for autofluorescence (3,4). In fluorescence microscopy, several parameters, such as excitation wavelengths, excitation power, microscope apertures, and buffers, have been optimized to minimize autofluorescence (5). However, autofluorescence cannot be fully eliminated in this way. Probably the most sophisticated method to eliminate autofluorescence is time-resolved fluorometry. This procedure is based on fluorescent lanthanide chelates with long decay times, which can be used to suppress the fast-decaying autofluorescence (6,7). This technique, however, needs a sophisticated fluorescence microscope to visualize the time-resolved emission (7).

Autofluorescence cannot be avoided by simply choosing a fluorescent probe with excitation and emission spectra out of the range of the spectra of autofluorescent molecules, because these spectra are very broad. In contrast, the spectra of fluorescent probes are relatively narrow. We have used these characteristics to develop a procedure to obtain an autofluorescence-free image. Signals were recorded at two excitation wavelengths, one signal representing both the specific fluorescence and the autofluorescence, and one signal representing only the autofluorescence. Subtraction of the latter signal from the former results in an autofluorescence-free image. The extent of autofluorescence is positively correlated with the section thickness and can be used to correct the specific fluorescence for section thickness.

Materials and Methods

Materials. Human lung tissue was obtained after lobectomy from a 56-year-old man; human quadriceps muscle was obtained at biopsy from a 41-year-old man; human heart tissue was obtained at autopsy 4 hr after death of a 41-year-old man; and rat quadriceps muscle was from a 3-month-old male Wistar rat.

Bovine serum albumin (BSA), rabbit anti-chicken gizzard desmin IgG, fluorescein isothiocyanate (FITC)-conjugated rabbit anti-mouse Ig antibodies, and FITC-conjugated goat anti-rabbit IgG antibodies were obtained from Sigma (St Louis, MO). Mouse monoclonal anti-heparan sulfate (JM403) antibody was a generous gift from Dr. J. van den Born (Dept. of Nephrology, University of Nijmegen), and was described previously (8). Mouse monoclonal antibody 3H6 is a self-developed antibody and is reactive with intercalated disks in human heart tissue.

¹ Supported by a grant from the Dutch Asthma Foundation (project no. 89.14).

² Correspondence to: T.H. van Kuppevelt, Dept. of Biochemistry, U. of Nijmegen, PO Box 9101, 6500 HB Nijmegen, The Netherlands.

Immunostaining. For indirect immunofluorescence, tissue samples were frozen in isopentane cooled with liquid nitrogen and stored at -70°C . Cryosections ($2\text{--}12\ \mu\text{m}$) were stored at -70°C . Cryosections were rehydrated for 10 min in PBS, pH 7.4, and primary and secondary antibodies were applied for 90 min in PBS containing 1% BSA. After each incubation, sections were washed in PBS (three times for 5 min). Anti-heparan sulfate antibody and FITC-conjugated secondary antibodies were used at a dilution of 1:100. Anti-desmin and 3H6 antibodies were used at a dilution of 1:50. In sections of quadriceps muscle, autofluorescence was enhanced by incubation with 3% formaldehyde in 150 mM phosphate buffer (pH 7.2) for 1 hr (1).

Comparison of Sections on the Basis of Protein Content. Because the micrometer setting of a microtome is not an accurate way to obtain sections of a certain thickness, we measured section thickness also by determining the surface and the protein content of a section. Sections were checked for homogeneity, i.e., for the presence of the same structural elements in the sections. This was done to exclude the possibility that sections differed from each other in structural composition, which may give rise to differences in measurable protein per unit of volume. Only sections consisting almost completely of muscle cells were taken. The surface of a cryosection was marked with a marker pen and copied by a photocopier onto a piece of paper. The image of the sections was cut out and weighed. The surface was calculated by using the weight of $1\ \text{cm}^2$ of paper as a standard. After surface analysis, the tissue section was taken up in demineralized water and the protein content was determined according to Lowry et al. (9). The section thickness was expressed in $\mu\text{g protein}/\text{mm}^2$.

Digital Subtraction of Autofluorescence. Microscopic (fluorescence) images were digitized using the MagiCal hardware and TARDIS software of Joyce-Loebl (Gateshead, UK). Images were captured with a resolution of 256×256 datapoints and 256 gray levels each. The images were processed with ImageCalc, an MS-Windows application designed for this purpose (10).

To subtract the autofluorescence signal, two images were digitized. For an FITC-immunostained tissue section, one image, representing the total fluorescence image (i.e., the specific FITC image plus the autofluorescence image), was obtained by excitation at 480 nm and emission at 515 nm. The second image, representing the autofluorescence image, was obtained by excitation at 380 nm and emission at 515 nm. For optimal results, two additional background images were digitized using the same parameters and representing images of an object slide without tissue. These images were used for noise and shading correction (11). Camera gain and sensitiv-

ity were adjusted to obtain optimal signal-to-noise ratios for both excitation wavelengths. Both images were captured immediately after each other, each image representing the average of eight individual images (to reduce noise). Total image capture of both images was achieved within 1 sec.

Because autofluorescence intensity depends on the excitation and emission wavelength utilized, a correction factor for the use of two wavelengths was applied by excitation of a non-immunostained cryosection at 480 and 380 nm. After determining the ratio of emission at 515 nm for these wavelengths ($R_{480/380}$) the specific fluorescence can be calculated using the equation:

$$\text{SF} = \text{TF} - (R_{480/380} \times \text{AF}),$$

where SF is the specific fluorescence, TF is the total fluorescence, and AF is the autofluorescence.

Results

Elimination of Autofluorescence

Human Lung Parenchyma. Human lung parenchyma sections display a very strong autofluorescence, mainly caused by elastin fibers (12). This autofluorescence masked the linear heparan sulfate basement membrane staining with antibody JM403 (Figure 1A), which was clearly visible on glomerular and tubule basement membranes (8). Digital subtraction of the autofluorescence image (Figure 1B) from the total fluorescence image revealed an autofluorescence-free image (Figure 1C). In this image, the linear basement membrane staining was clearly visible. The autofluorescence image lacked any specific basement membrane staining.

Human Heart Muscle. Human heart muscle, especially from individuals of older age, contains the strongly autofluorescent pigment lipofuscin (13). Immunostaining of heart tissue sections with monoclonal antibody 3H6 showed staining of the intercalated disks. This staining, however, was locally completely masked by the autofluorescent lipofuscin particles (Figure 2A). Subtraction of the autofluorescence image (Figure 2B) unmasked the specific staining of the intercalated disks (Figure 2C).

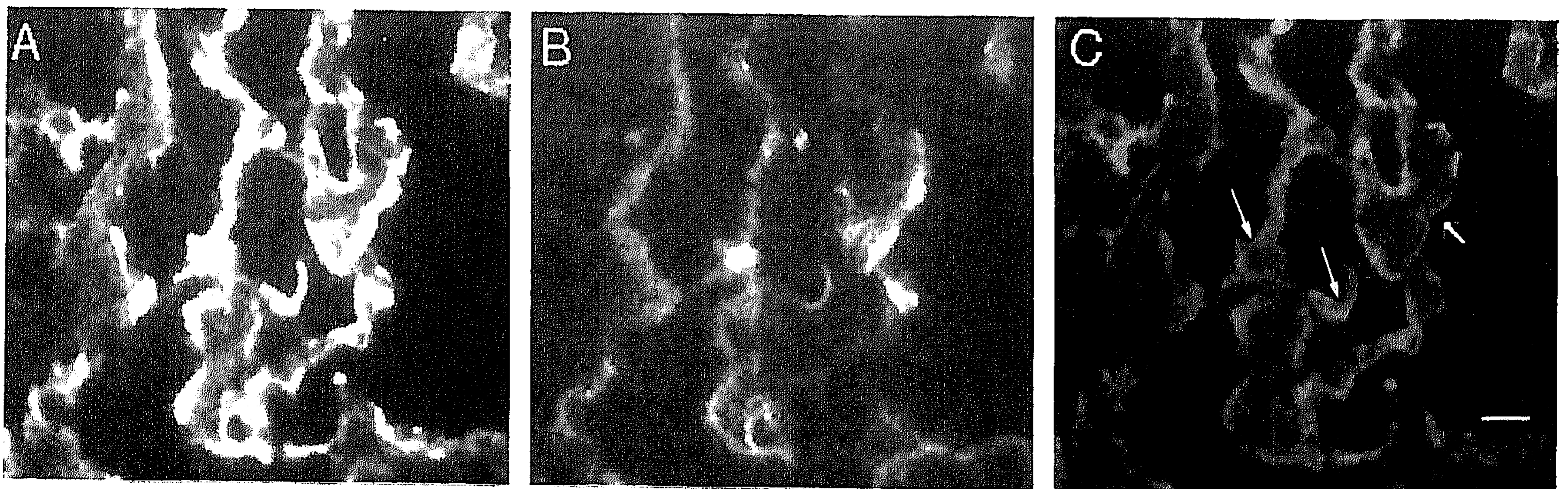


Figure 1. Elimination of autofluorescence (mainly caused by elastin fibers) in human lung parenchyma sections. Sections were stained with mouse anti-heparan sulfate antibodies, which were detected with FITC-labeled rabbit anti-mouse Ig antibodies. The autofluorescence image (B) was subtracted from the total fluorescence image (A), resulting in an autofluorescence-free image (C). Arrows indicate areas where the basement membrane location of heparan sulfate becomes visible only after subtraction of autofluorescence. The correction factor $R_{480/380}$ was 0.7. Bar = $25\ \mu\text{m}$.



Figure 2. Elimination of autofluorescence caused by lipofuscin in human heart sections. Tissue sections were immunostained with the mouse monoclonal antibody 3H6, which is reactive with intercalated disks. Antibodies were detected with FITC-labeled rabbit anti-mouse Ig antibodies. The total fluorescence image (A) minus the autofluorescence image (B) results in an autofluorescence-free image (C) completely lacking the fluorescence of lipofuscin particles. Note that the specific fluorescence at some intercalated disks becomes visible only after elimination of autofluorescence (arrow). The correction factor $R_{480/380}$ was 1.0. Bar = 25 μm .

Use of Autofluorescence as a Measure of Tissue Thickness

Because the autofluorescence signal can be obtained separately, we investigated if the intensity of this signal could be used as a measure of the thickness of a section. Since this requires an equal distribution of autofluorescence over the section, we used sections of quadriceps muscle in which the autofluorescence was enhanced by pre-incubation with formaldehyde. To obtain precise measurements, the section thickness was accurately measured by analysis of surface and protein content. We found a positive correlation between the section thickness (measured as $\mu\text{g protein}/\text{mm}^2$) and the autofluorescence intensity (Figure 3). We evaluated this observation further on sections of human quadriceps muscle stained with anti-desmin antibodies. Whereas the specific fluorescence and the auto-

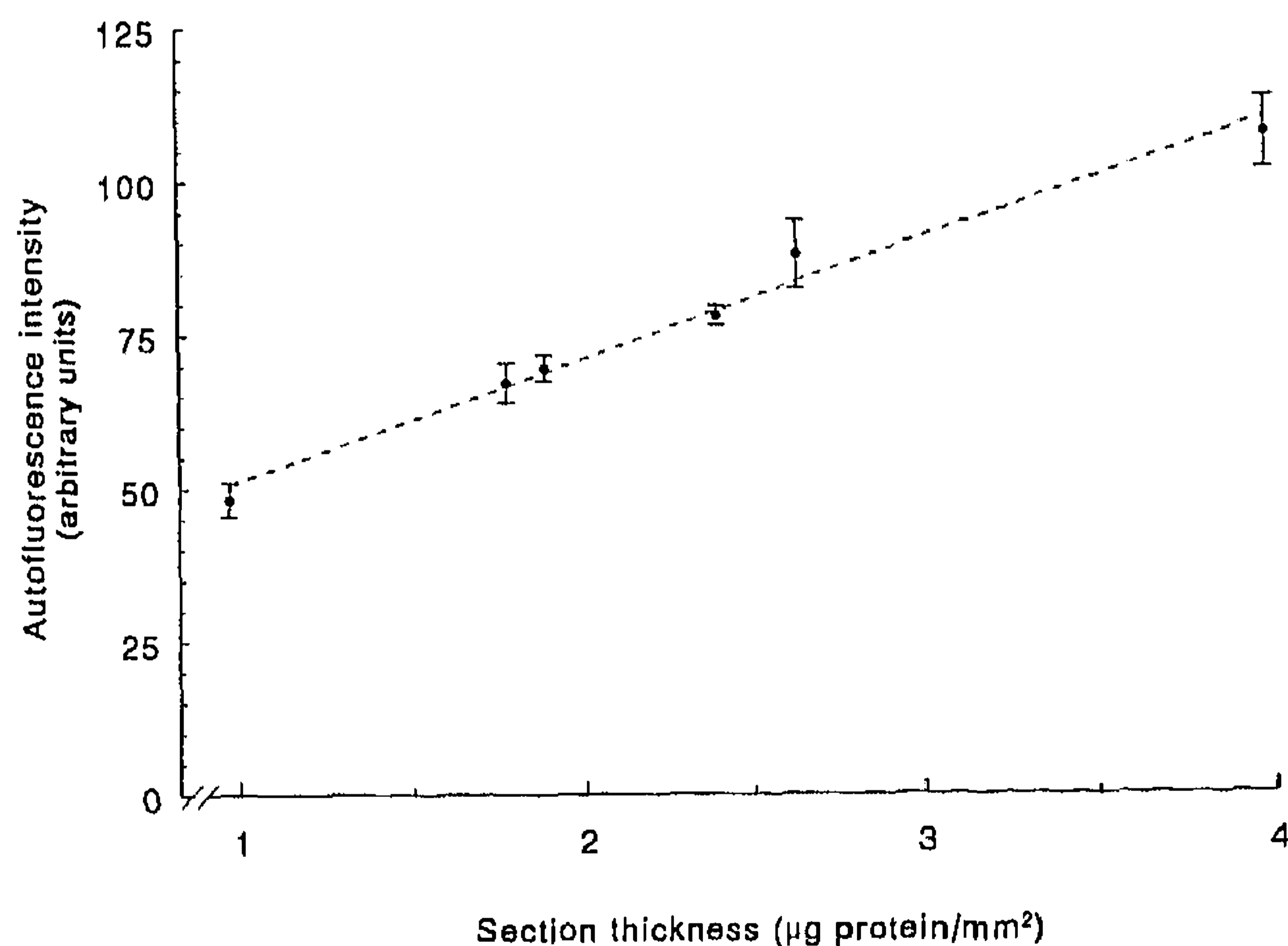


Figure 3. Autofluorescence as a measure of section thickness. Autofluorescence was established in sections of rat quadriceps muscle with various thickness (expressed as $\mu\text{g protein}/\text{mm}^2$). Autofluorescence was enhanced by pre-incubation of the sections with formaldehyde. Values are mean \pm SEM of four individual observations. Note that there is a positive correlation ($r = 0.93$; $p < 0.0001$) between autofluorescence and section thickness.

fluorescence showed a clear correlation with the apparent thickness of the sections (indicated by the microtome), the ratio between these fluorescence parameters was independent of the apparent section thickness (Figure 4).

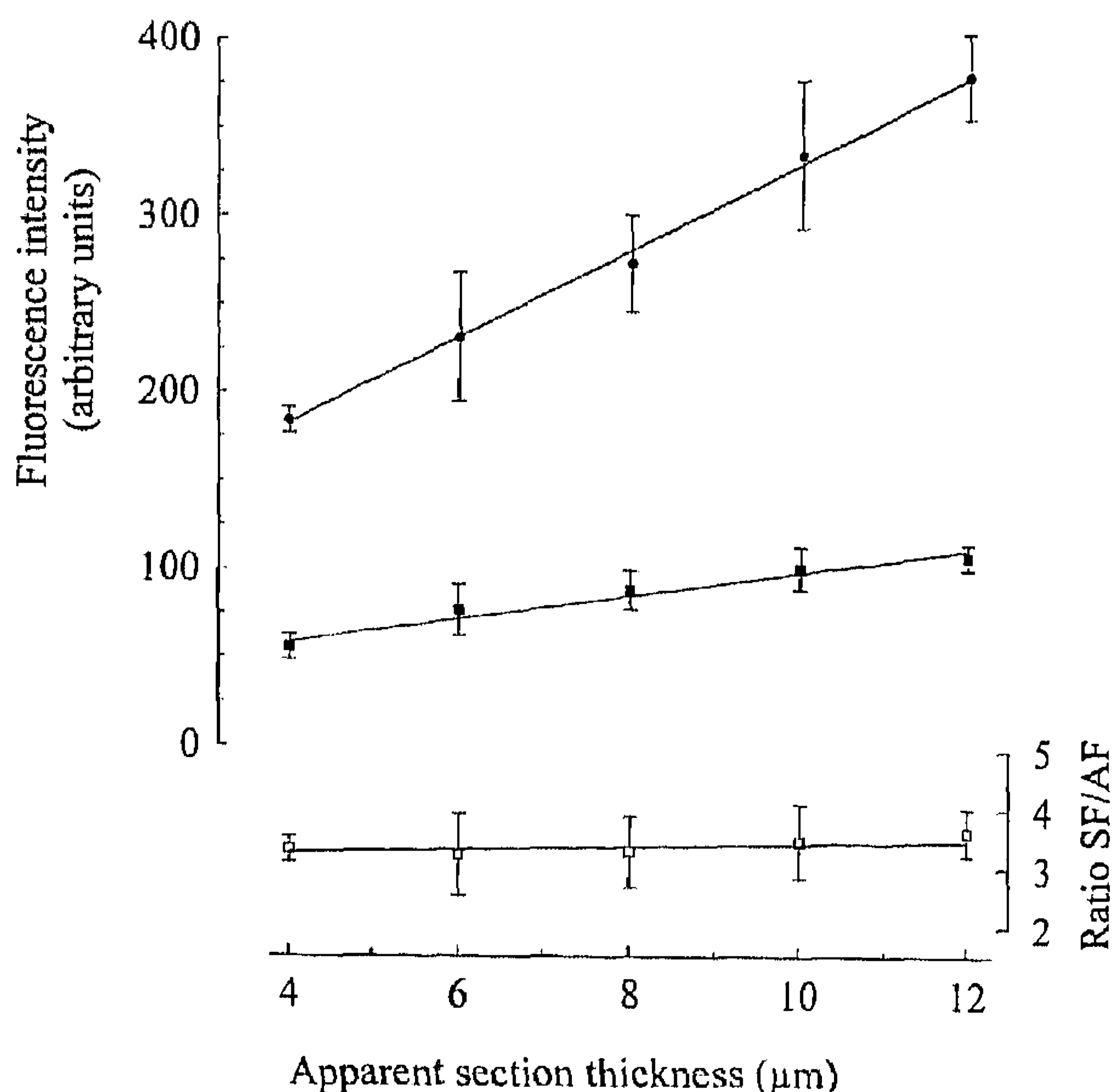


Figure 4. The specific fluorescence (●), the autofluorescence (■), and the ratio of specific fluorescence and autofluorescence (□) as a function of the apparent thickness of sections of human quadriceps muscle stained with rabbit anti-chicken desmin antibodies and FITC-labeled goat anti-rabbit IgG antibodies. Section thickness was derived from the microtome setting. A positive correlation is present between both the specific fluorescence and the autofluorescence and the apparent section thickness ($r = 0.69$, $p < 0.001$; $r = 0.51$, $p < 0.01$, respectively). The ratio of specific fluorescence (SF) and autofluorescence (AF) is independent of the thickness of the sections ($r = 0.21$; $p < 0.7$). Autofluorescence was enhanced by pre-incubation of the sections with formaldehyde. Values are mean \pm SEM of four individual observations.

Discussion

In this report we demonstrate that autofluorescence in immunofluorescence microscopy can be efficiently eliminated by subtraction of the autofluorescence image, captured using an excitation wavelength outside the excitation spectrum of the fluorophore. This principle has been used for elimination of autofluorescence in flow cytometry (3,4), and we show here that it is also applicable in immunofluorescence microscopy of tissue sections. Using this technique, we were able to eliminate the strong autofluorescence of elastin and lipofuscin without affecting the specific fluorescence. An alternative way to eliminate autofluorescence is time-delayed fluorometry (6). This procedure, however, needs a sophisticated and expensive fluorescence microscope (7), whereas our technique requires only a digitization apparatus (e.g., a CCD camera) connected to a standard fluorescence microscope.

Elimination of autofluorescence can simplify the interpretation of immunostained sections, especially in tissues with an abundance of autofluorescent molecules, such as heart and brain (lipofuscin) and lung (elastin). The method is also useful in cases where the specific staining is weak (e.g., in tissues with a small amount of antigen or in situ hybridization). Because the digitization process is usually performed within a single second, fading of the fluorescent probe is minimized, which is essential for quantitative analysis (14). In addition, specific fluorescence can be corrected for section thickness using the autofluorescence signal (Figure 4).

In conclusion, autofluorescence in tissue sections treated for immunofluorescence microscopy can be effectively eliminated by digitalization of the fluorescence signal at two different wavelengths. Correction for section thickness and minimal fading of the fluorophore make this method suitable for (semi)quantitative analysis of stained sections.

Acknowledgment

We are indebted to Dr A. Benders for excellent assistance with the MagiCal digital image analyzer.

Literature Cited

1. Falck B, Owman J. Formaldehyde induced fluorescence. *Acta Univ Lund* 1965 (sect II:7)
2. Hallden G, Skold CM, Eklund A, Forslid J, Hed J. Quenching of intracellular autofluorescence in alveolar macrophages permits analysis of fluorochrome labelled surface antigens by flow cytometry. *J Immunol Methods* 1991;142:207
3. Steinkamp JA, Stewart CC. Dual-laser, differential fluorescence correction method for reducing cellular background autofluorescence. *Cytometry* 1986;7:566
4. Pankow W, Newmann K, Ruschoff J, Heymanns J, Von Wichert P. A cytofluorometric method to quantify membrane antigens on individual alveolar macrophages. *J Immunol Methods* 1990;129:127
5. Noonberg SB, Weiss TL, Garovoy MR, Hunt CA. Characterization and minimization of cellular autofluorescence in the study of oligonucleotide uptake using confocal microscopy. *Antisense Res Dev* 1992;2:303
6. Seveus L, Vaisala M, Syrjanen S, Sandberg M, Kuusisto A, Harju R, Salo J, Hemmila I, Kojola H, Soini E. Time-resolved fluorescence imaging of europium chelate label in immunohistochemistry and in situ hybridization. *Cytometry* 1992;13:329
7. Marriott G, Clegg RM, Arndt Jovin DJ, Jovin TM. Time resolved imaging microscopy. Phosphorescence and delayed fluorescence imaging. *Biophys J* 1991;60:1374
8. Van den Born J, Van den Heuvel LPWJ, Bakker MAH, Veerkamp JH, Assmann KJM, Berden JHM. A monoclonal antibody against GBM heparan sulfate induces an acute selective proteinuria in rats. *Kidney Int* 1992;41:115
9. Lowry OH, Rosenbrough NJ, Farr AL, Randall RJ. Protein measurement with the Folin phenol reagent. *J Biol Chem* 1951;193:265
10. Van de Lest CHA, Veerkamp JH, Van Kuppevelt TH. *ImageCalc* [computer program]. Version 1.1. Nijmegen, The Netherlands: Department of Biochemistry, Faculty of Medicine, University of Nijmegen, 1995. 1 computer disk. System requirements: IBM or compatible 386 SX or higher; 4 Mb RAM; minimum hard disk space 1 Mb; MS Windows 3.1; 256-color graphics adaptor. This program can be obtained from our lab by sending a blank MS-DOS-formatted diskette (5.25" or 3.5" high or double density) with a self-addressed envelope. The program is released as shareware and may be used only for non-commercial purposes. If you find the program useful, we ask you to support the Dutch Asthma Foundation with a contribution of at least \$25.00.
11. Boone JM, Seibert JA, Barrett WA, Blood EA. Analysis and correction of imperfections in the image intensifier-TV-digitizer imaging chain. *Med Phys* 1991;18:236
12. Mauderly JL, Bice DE, Cheng YS, Gillett NA, Henderson RF, Pickrell JA, Wolff RK. Influence of experimental pulmonary emphysema on the toxicological effects from inhaled nitrogen dioxide and diesel exhaust. *Res Rep Health Eff Inst* 1989;1
13. Harman D. Lipofuscin and ceroid formation: the cellular recycling system. *Adv Exp Med Biol* 1989;266:3
14. Enerback L, Johansson KA. Fluorescence fading in quantitative fluorescence microscopy: a cytofluorometry of the automatic recording of fluorescence peaks of very short duration. *Histochem J* 1973;5:351